

Emission analysis of Pr³⁺ & Dy³⁺ ions doped Li₂O-LiF-B₂O₃-ZnO glasses

L. Vijayalakshmi*, V. Naresh, B.H. Rudramadevi & S. Buddhudu⁺
⁺Dept. of Physics, Sri Venkateswara University, Tirupati-517502.

ABSTRACT: The present paper reports on the optical and spectral results of (0.5 mol %) Pr³⁺ or (0.5 mol %) Dy³⁺ ions containing Li₂O-LiF- B₂O₃-ZnO (LBZ) glasses were prepared by a melt quenching technique. These glasses have shown strong absorption bands in visible and near infrared (NIR) regions. Pr³⁺: LBZ glass has exhibited six emission bands in the visible region at ³P₀→³H₄ (490 nm), ³P₁→³H₅ (532 nm), ¹D₂→³H₄ (608 nm), ³P₀→³F₂ (652 nm), ³P₀→³F₃ (690 nm) and ³P₀→³F₄ (723 nm) on exciting at 446 nm (³H₄→³P₂) and a broad emission band ¹D₂→¹G₄ (1.46 μm) in the NIR region upon exciting with Ar+ laser (514.5 nm). In the case of Dy³⁺: LBZ glass, three emission bands are observed attributed to the transitions ⁴F_{9/2}→⁶H_{15/2} (486 nm), ⁴F_{9/2}→⁶H_{13/2} (577 nm) and ⁴F_{9/2}→⁶H_{11/2} (662 nm) with an excitation 385 nm (⁶H_{15/2}→⁶I_{13/2}). The emission process has been explained from their energy level diagrams. Besides these, emission decay curves have been plotted for these prominent emission bands, in order to evaluate their emission lifetimes (τ).

KEYWORDS: Melt quenching method; optical glasses & luminescence.

I. INTRODUCTION

Luminescent host matrices like glasses, ceramics, glass ceramics and phosphors containing rare-earth or transition metal ions have gained much importance in the progress of optical materials of significant importance. Among those, glasses are attractive materials because of their physical, electrical and optical applications in the fields of optoelectronics, photonics & optical fibre communications [1-5]. Oxy-fluoro borate glasses have been identified as good glassy materials due to their good glass forming ability, hardness, transparency and resistance towards the moisture and with an extended IR transmission ability [3, 6-8]. In order to improve the glass quality and its optical performance a divalent oxide such as ZnO has been added separately besides the other property improving network modifier (NWM) namely Li₂O. Rare earth ions Pr³⁺ and Dy³⁺ ions incorporated glasses have received more attention because of their potential applications in optical communication and in display devices [5, 9-12]. These two rare-earth (Pr³⁺ or Dy³⁺) ions show narrow and intense absorption bands in the NIR region and interesting emissions in the reddish-orange and blue/yellow colours under an UV excitation source. Therefore, these ions are incorporated into the Li₂O-LiF- B₂O₃-ZnO (LBZ) glass matrix in order to understand the optical and spectral properties of Pr³⁺ and Dy³⁺ glasses systematically.

II. EXPERIMENTAL STUDIES

2.1 Glass sample preparation

The glass samples studied in the present work were prepared by melt quenching method. The chemical compositions (all are in wt%) of the host glass with and without transition metal ions are taken in the following chemical composition:

- (i) 30Li₂O-20LiF-45B₂O₃-5ZnO (LBZ host glass)
- (ii) 30Li₂O-20LiF-45.5B₂O₃-4ZnO-0.5 mol% Pr₂O₃ (0.5 Pr³⁺ : LBZ glass)
- (iii) 30Li₂O-20LiF-45.5B₂O₃-4ZnO-0.5 mol% Dy₂O₃ (0.5 Dy³⁺ : LBZ glass)

The starting chemicals were used were in analytical grade such as H₃BO₃, Li₂CO₃, LiF, ZnCO₃, Pr₂O₃ and Dy₂O₃. All the chemicals were weighed in 10g batch each separately, thoroughly mixed and finely powdered using an agate mortar and pestle and each of those was collected into a porcelain crucible and heated gradually in an electric furnace for melting them for an hour at 950°C. These melts were quenched in between two smooth surfaced brass plates to obtain glasses in circular designs with 2-3 cm in diameter and a thickness of 0.3 cm. Thus, obtained glass sample were carried to have further characterizations.

2.2. Measurements

The excitation and emission spectra of singly doped Pr^{3+} , Dy^{3+} glasses were recorded at room temperature on a *SPEX Fluorolog-3 (Model-II)* spectrophotometer, attached with an Xe-arc lamp (450 W) as the excitation source. This system is employed with a Datamax software package for acquiring the spectral data and decay-curve (lifetime measurement) data using a phosphorimeter and a Xe-flash lamp. NIR photoluminescence spectra of Pr^{3+} : LBZ glass is measured on a Horiba Triax-550 grating monochromator (JOBIN YVON HORIBA) equipped with a liquid nitrogen cooled InGaAS photodetector (electro-optical system Inc.) in the wavelength range 800-1700 nm and a lock-in-amplifier (SR 830 DSP, Standard Research System) attached with an Ar^+ laser (514.5 nm) (Lexel Model 85 Ion Laser, 5Mw-200mW) as an excitation source.

III. RESULTS AND DISCUSSION

3.1 Absorption and luminescence properties of Pr^{3+} : LBZ glass

Fig. 1 shows the optical absorption spectrum of Pr^{3+} :LBZ glass displaying a series of absorption bands assigned to electronic transitions originating from ground state $^3\text{H}_4$ to $^3\text{P}_2$ (441 nm), $^3\text{P}_1+^1\text{I}_6$ (471 nm), $^3\text{P}_0$ (481 nm), $^1\text{D}_2$ (589 nm), $^3\text{F}_4$ (1413 nm), $^3\text{F}_3$ (1516 nm). Of all these, $^3\text{H}_4 \rightarrow ^3\text{P}_2$ transition is hypersensitive in nature and governed by the selection rules $\Delta S = 0$, $\Delta L \leq 2$ and $\Delta J \leq 2$ [14-16].

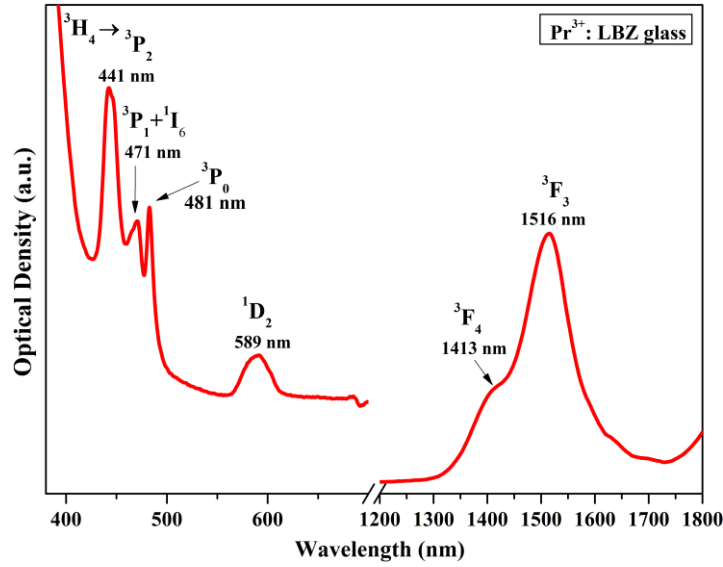


Fig. 1: Optical absorption spectrum of Pr^{3+} : LBZ glass

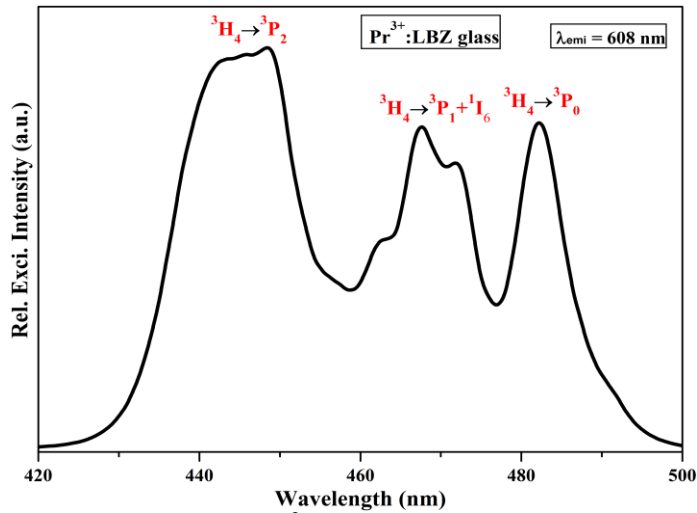


Fig. 2: Excitation spectrum of Pr^{3+} : LBZ glass with an $\lambda_{\text{emi}} = 608 \text{ nm}$

Excitation spectrum of 0.5 mol % Pr^{3+} : LBZ glass is shown in the Fig.2, exhibiting electronic transitions $^3\text{H}_4 \rightarrow ^3\text{P}_2$, $^3\text{H}_4 \rightarrow ^3\text{P}_1+^1\text{I}_6$ and $^3\text{H}_4 \rightarrow ^3\text{P}_0$ on monitoring with 608 nm ($^1\text{D}_2 \rightarrow ^3\text{H}_4$). Among the excitation bands, the prominent band at 446 nm ($^3\text{H}_4 \rightarrow ^3\text{P}_2$) has been chosen to measure the emission spectrum of 0.5 mol % Pr^{3+} : LBZ glass in the visible region as shown in the Fig. 3(a). The emission spectrum of Pr^{3+} glass has demonstrated six emission transitions at $^3\text{P}_0 \rightarrow ^3\text{H}_4$ (490 nm; yellow), $^3\text{P}_1 \rightarrow ^3\text{H}_5$ (532 nm; green), $^1\text{D}_2 \rightarrow ^3\text{H}_4$ (608 nm; orange), $^3\text{P}_0 \rightarrow ^3\text{F}_2$ (652 nm; red), $^3\text{P}_0 \rightarrow ^3\text{F}_3$ (690 nm; red) and $^3\text{P}_0 \rightarrow ^3\text{F}_4$ (723 nm; red) upon exciting at 446 nm ($^3\text{H}_4 \rightarrow ^3\text{P}_2$) [14-18]. Up on exciting at 446 nm, Pr^{3+} ions in the ground state are excited to the higher energy states later on these ions decay non-radiatively to next lower states of $^3\text{P}_1$, $^3\text{P}_0$ and to $^1\text{D}_2$. Therefore ions in $^3\text{P}_1$ state decay radiatively to the $^3\text{H}_5$ state. The $^3\text{P}_0$ excited state transfer these populated ions non-radiatively to nearby $^1\text{D}_2$ state and radiatively to lower lying $^3\text{F}_j$ and $^3\text{H}_j$ states with the ejection of corresponding emissions.

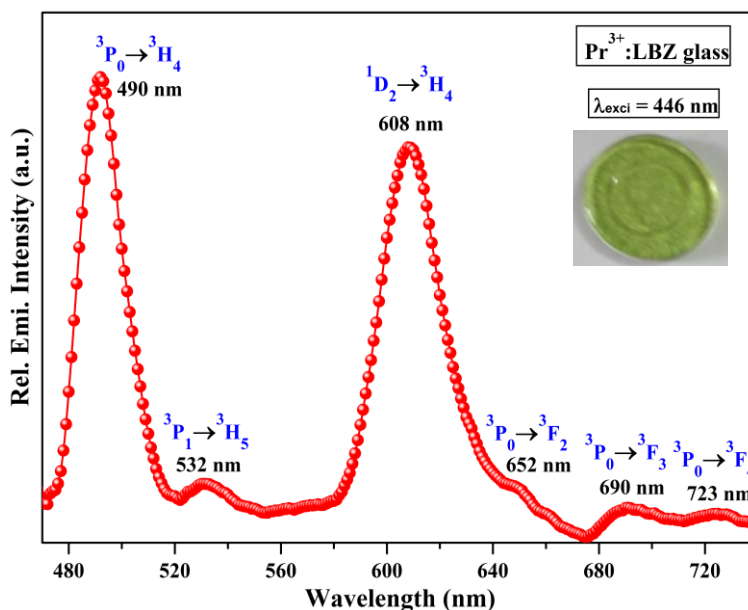


Fig. 3(a): Visible emission spectrum of Pr^{3+} : LBZ glass with $\lambda_{\text{exci}} = 446$ nm

The NIR emission spectrum of Pr^{3+} : LBZ glass is shown in Fig.3 (b). On exciting with Ar^+ laser as an excitation source at 514.5 nm, the fluorescence spectrum has exhibited a broad emission band at 1.46 μm assigned to electronic transition $^1\text{D}_2 \rightarrow ^1\text{G}_4$ which covers E to U bands useful in optical fiber communication. The NIR emission spectrum of Pr^{3+} : LBZ glass is shown in Fig.3 (b).

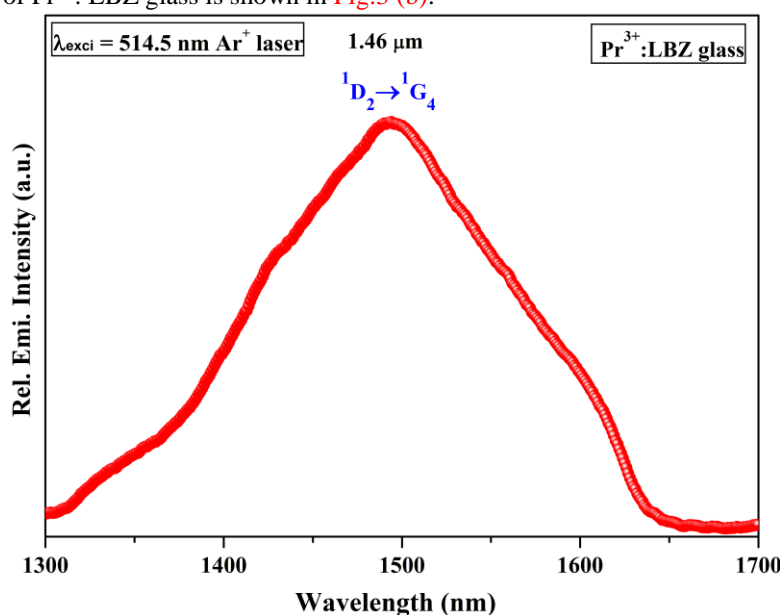


Fig. 3(b): NIR emission spectrum of Pr^{3+} : LBZ glass with $\lambda_{\text{exci}} = 514.5$ nm

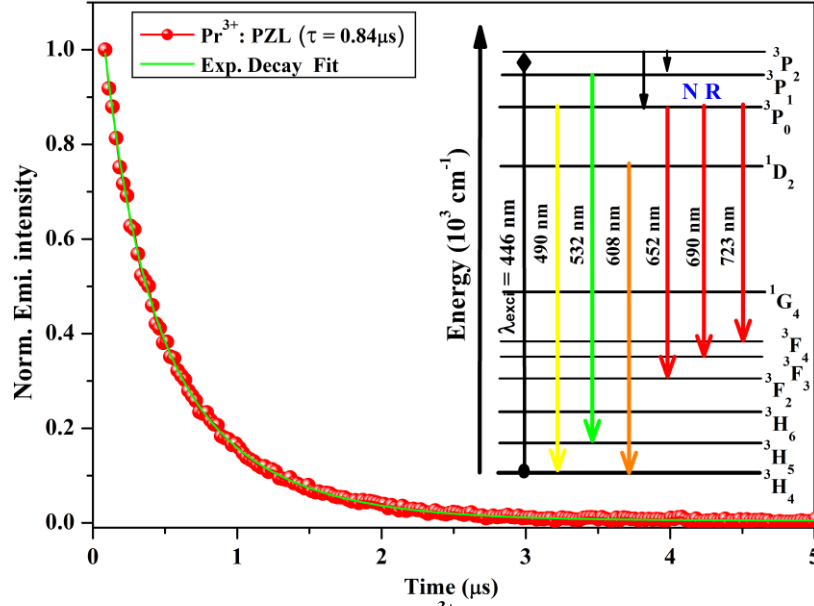


Fig. 4: Emission decay curve of Pr^{3+} : LBZ glass for $\lambda_{\text{emi}} = 608 \text{ nm}$

On exciting with Ar^+ laser as an excitation source at 514.5 nm, the fluorescence spectrum has exhibited a broad emission band at 1.46 μm assigned to electronic transition $^1\text{D}_2 \rightarrow ^1\text{G}_4$ which covers E to U bands useful in optical fiber communication. Fig.4 represents emission decay curve for Pr^{3+} glass for prominent emission $^1\text{D}_2 \rightarrow ^3\text{H}_4$ (608 nm) with $\lambda_{\text{exci}} = 446 \text{ nm}$. The lifetime has been evaluated to be 0.84 μs . The emission mechanism taking place between the energy levels is explained from energy level diagram as shown in inset of Fig.4.

3.2 Absorption and luminescence properties of Dy^{3+} : LBZ glass

In Fig.5, absorption of Dy^{3+} : LBZ glass is shown exhibiting absorption bands that originate from the ground state $^6\text{H}_{15/2}$ to various excited states $^4\text{I}_{13/2}$ (386 nm), $^4\text{G}_{11/2}$ (425 nm), $^4\text{I}_{15/2}$ (452 nm), $^4\text{F}_{9/2}$ (476 nm), $^6\text{F}_{3/2}$ (742 nm), $^6\text{F}_{5/2}$ (801 nm), $^6\text{F}_{7/2}$ (898 nm), $^6\text{F}_{9/2}$, $^6\text{H}_{7/2}$ (1088 nm), $^6\text{F}_{11/2}$, $^6\text{H}_{9/2}$ (1261 nm), $^6\text{H}_{13/2}$ (1674 nm) respectively.

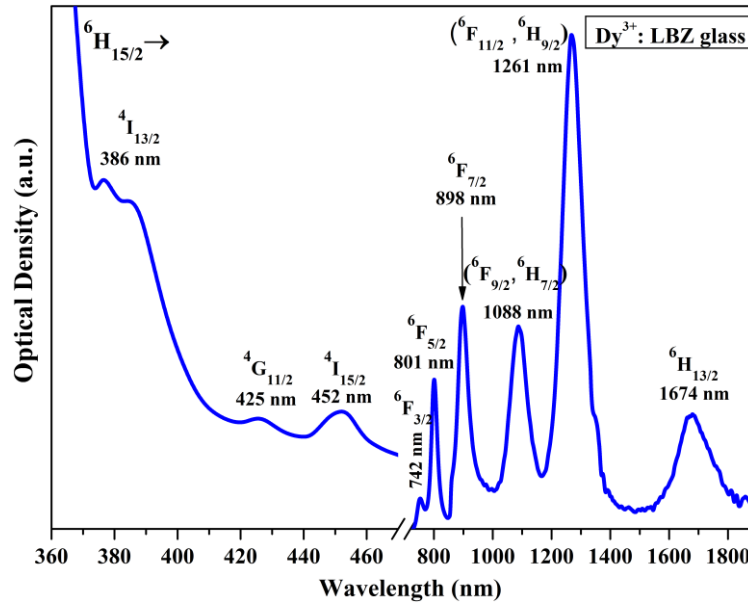


Fig. 5: Optical absorption spectrum of Pr^{3+} : LBZ glass

Most of the absorption transitions of Dy^{3+} originate based on the selection rules $|\Delta L| \geq 0$, $|\Delta J| \geq 0$ and $|\Delta S| = 0$. The high intense transitions in the infrared region are spin allowed ($\Delta S = 0$) and the transitions in the visible region are spin-forbidden [19-24].

Fig.6 (a) & (b) present the excitation and emission spectra of (0.5 mol %) Dy^{3+} : LBZ glass. The excitation spectra consists of 6 bands at 325 nm, 350 nm, 365 nm, 385 nm, 425 nm, and 452 nm attributed to the transitions from ${}^6H_{15/2}$ to ${}^4P_{3/2}$, ${}^4I_{15/2}$, ${}^4I_{11/2}$, ${}^4I_{13/2}$, ${}^4G_{11/2}$ and ${}^4I_{15/2}$ of Dy^{3+} .

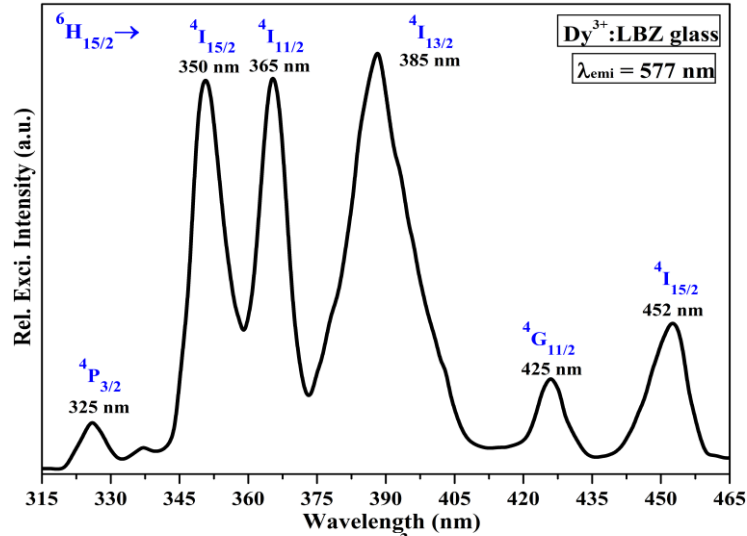


Fig. 6(a): Excitation spectrum of Dy^{3+} : LBZ glass with $\lambda_{emi} = 577$ nm

Of these transitions ${}^6H_{15/2} \rightarrow {}^6I_{13/2}$ (385nm) is more prominent, it is therefore used for the measurement of emission spectra of Dy^{3+} :LBZ glass. Dy^{3+} ions are excited to ($4f^85d$) upper energy level under an excitation with 385 nm and from where these excited ions cascade rapidly towards ${}^4F_{9/2}$ state through ${}^4G_{11/2}$, ${}^4I_{15/2}$ levels and then finally relaxes non-radiatively by populating ${}^4F_{9/2}$ metastable state. The non-radiative decay is very fast because of closely spaced $4f^9$ levels between ${}^4F_{9/2}$ and $4f^85d$ levels. On reaching ${}^4F_{9/2}$ level these unstable ions relax radiatively by emitting fluorescence to the nearest lower lying multiplet 6H_J ($J = 15/2, 13/2, 11/2$) energy level. The fluorescence spectrum exhibited two main peaks at 486 nm, 577 nm and with a weak band at 662 nm assigned to transitions of ${}^4F_{9/2} \rightarrow {}^6H_{15/2}$, ${}^6H_{13/2}$, and ${}^6H_{11/2}$. The intensity of ${}^4F_{9/2} \rightarrow {}^6H_{15/2}$ (486 nm; Blue) emission is stronger than that of ${}^4F_{9/2} \rightarrow {}^6H_{13/2}$ (577 nm; Yellow) and ${}^4F_{9/2} \rightarrow {}^6H_{11/2}$ (662 nm; Red) emissions. The blue emission at ${}^4F_{9/2} \rightarrow {}^6H_{15/2}$ is a magnetic dipole ($\Delta J = 0, \pm 1$ but $0 \leftrightarrow 0$ is forbidden) transition which hardly varies with the host glass environment around Dy^{3+} ion. The yellow emission due to ${}^4F_{9/2} \rightarrow {}^6H_{13/2}$ transition is a forced electric dipole transition (hypersensitive) with the selection rule $\Delta J = \pm 2$ and it is strongly influenced by the crystal field strength around the rare earth ion and red emission at 662 nm assigned to ${}^4F_{9/2} \rightarrow {}^6H_{11/2}$ transition is an electric dipole allowed.

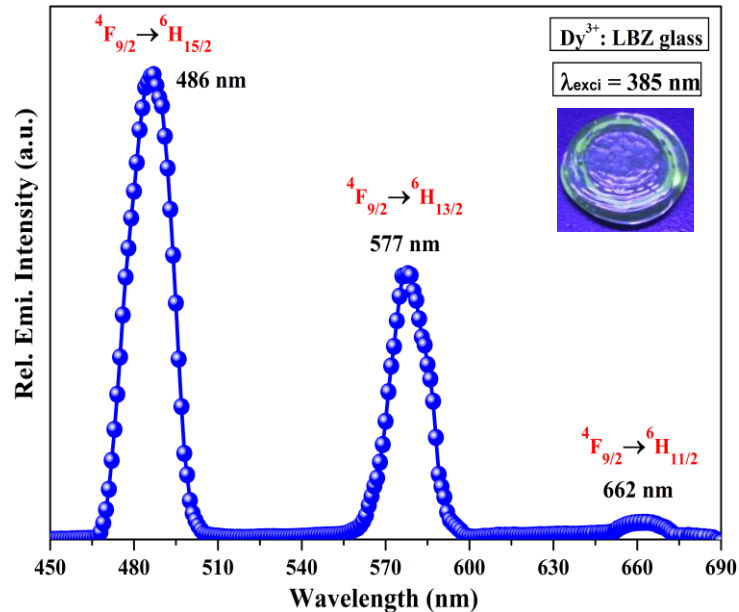


Fig. 6(b): Visible emission spectrum of Dy^{3+} : LBZ glass with $\lambda_{exc} = 385$ nm

When Dy^{3+} occupies a non-inversion symmetry site (low local symmetry site) yellow (${}^6\text{H}_{13/2}$; ED) emission is more dominant and if it occupies an inversion symmetry site (high symmetry local site) blue (${}^6\text{H}_{15/2}$; MD) emission is more dominant in the emission spectrum [19-24]. In the present work, ${}^4\text{F}_{9/2} \rightarrow {}^6\text{H}_{13/2}$ (ED) transition is less intense compared to ${}^4\text{F}_{9/2} \rightarrow {}^6\text{H}_{15/2}$ (MD) transition suggesting the symmetric nature of Dy^{3+} in the host glass. The intensity ratio of yellow/blue emission can be used to analyze the distortion around the Dy^{3+} ion in the glass matrices.

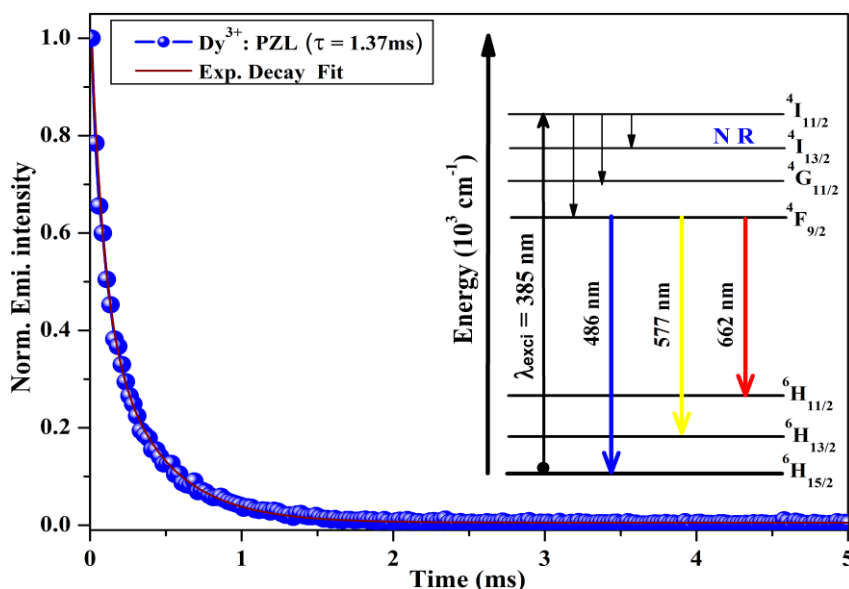


Fig. 4: Emission decay curve of Pr^{3+} : LBZ glass for $\lambda_{\text{emi}} = 577 \text{ nm}$

Fig. 7, shows the emission decay curve for Dy^{3+} glass and the lifetime has been evaluated to be 1.37 ms. The emission mechanism taking place between the energy levels is explained from energy level diagram is inserted in Fig. 7.

IV. CONCLUSION

Pr^{3+} and Dy^{3+} ions doped $\text{Li}_2\text{O-LiF-B}_2\text{O}_3\text{-ZnO}$ (LBZ) glasses were prepared separately by employing melt quenching technique. Optical absorption and emission spectra of Pr^{3+} : LBZ and Dy^{3+} : LBZ glasses have been measured and systematically analyzed. Pr^{3+} glass exhibited two prominent emissions in the visible region assigned to the transitions ${}^3\text{P}_0 \rightarrow {}^3\text{H}_4$ (490 nm; blue), ${}^1\text{D}_2 \rightarrow {}^3\text{H}_4$ (608 nm, red) on exciting at 446 nm (${}^3\text{H}_4 \rightarrow {}^3\text{P}_2$) and a broad emission ${}^1\text{D}_2 \rightarrow {}^1\text{G}_4$ (1.46 μm) in the NIR region upon exciting with Ar+ laser (514.5 nm). With regard to emission spectrum of Dy^{3+} glass, it has demonstrated two prominent emission bands attributed to the electronic transitions of ${}^4\text{F}_{9/2} \rightarrow {}^6\text{H}_{15/2}$ (486 nm; blue), and ${}^4\text{F}_{9/2} \rightarrow {}^6\text{H}_{13/2}$ (577 nm, yellow) with an excitation 385 nm (${}^6\text{H}_{15/2} \rightarrow {}^6\text{I}_{13/2}$). Based on the emission characteristic features, such optical glasses could be suggested as potential materials for their use in the progress of optical lasers, photonic and optoelectronic devices

REFERENCES

- [1] Vogel, W. Chemistry of glass. 1985. *American Ceramic Society*, Westerville, Ohio.
- [2] D. Ehrt, Structure, properties and applications of borate glasses, *Glass Tech.* **41** (2000) 182.
- [3] V. Naresh, S. Buddhudu, Structural, thermal, dielectric and ac conductivity properties of lithium fluoro-borate optical glasses, *Ceram. Int.* **38** (2012) 2325.
- [4] R.S. Gedam, D.D. Ramteke, Electrical, dielectric and optical properties of La_2O_3 doped lithium borate glasses, *J. Phys. Chem. Solids* **74** (2013) 1039.
- [5] Bo Zhou, Lili Tao, Yuen H. Tsang, Wei Jin and Edwin Yue-Bun Pun, Superbroadband near-IR photoluminescence from Pr^{3+} -doped fluorotellurite glasses, *Opt. Express* **20** (2012) 3803.
- [6] W.A. Pisarski, T. Goryczka, B. Wodecka-Dus, M. Plonska, J. Pisarska, Structure and properties of rare earth-doped lead borate glasses, *Mater. Sci. Eng. B* **122** (2005) 94.
- [7] N. A. Minakova, A. V. Zaichuk and Ya. I. Belyi, The structure of borate glass, *Glass and Ceramics*, **65** (2008) 70.
- [8] Wojciech A. Pisarskia, Joanna Pisarskab, Witold Ryba-Romanowski, Structural role of rare earth ions in lead borate glasses evidenced by infrared spectroscopy: $\text{BO}_3 \rightarrow \text{BO}_4$ conversion, *J. Mol. Struct.* **744-747** (2005) 515.
- [9] G. Lakshminarayana, R. Vidya Sagar, S. Buddhudu, Emission analysis of Dy^{3+} and Pr^{3+} : $\text{Bi}_2\text{O}_3\text{-ZnF}_2\text{-B}_2\text{O}_3\text{-Li}_2\text{O-Na}_2\text{O}$ glasses, *Physica B* **403** (2008) 81.
- [10] F. Charpentier, F. Starecki, J.L. Doualan, P. Jovari, P. Camy, J. Troles, S. Belin, B. Bureau, and V. Nazabal, Mid-IR luminescence of Dy^{3+} and Pr^{3+} doped $\text{Ga}_5\text{Ge}_{20}\text{Sb}_{10}\text{S}(\text{Se})_{65}$ bulk glasses and fibers, *Mater. Lett.* **101** (2013) 21.
- [11] Martin Pavlista, Pavla Sourkova, Miloslav Frumar, Petr Nemecek, Electronic energy levels of trivalent lanthanide ions in chalcogenide glasses: Case of Pr^{3+} , Sm^{3+} and Dy^{3+} , *Mater. Lett.* **65** (2011) 3427.

- [12] G. Lakshminarayana, Jianrong Qiu, Photoluminescence of Pr³⁺, Sm³⁺ and Dy³⁺-doped SiO₂-Al₂O₃-BaF₂-GdF₃ glasses, *J. Alloy Compd.* **476** (2009) 470.
- [13] Liaolin Zhang, Guoping Dong, Mingying Peng, Jianrong Qiu, Comparative investigation on the spectroscopic properties of Pr³⁺-doped boro-phosphate, boro-germo-silicate and tellurite glasses, *Spectrochim. Acta A*, **93** (2012) 223.
- [14] Marcos P. Belancon, Jorge D. Marconi, Mariana F. Ando, Luiz C. Barbosa, Near-IR emission in Pr³⁺ single doped and tunable near-IR emission in Pr³⁺/Yb³⁺ codoped tellurite tungstate glasses for broadband optical amplifiers, *Opt. Mater.* **36** (2014) 1020.
- [15] D. Rajeswara Rao, G. Sahaya Baskaran, P. Ramesh Babu, Y. Gandhi, N. Veeraiah, Studies on optimizing sesquioxide contents to enhance luminescence efficiency of Pr³⁺ ions in PbOPbF₂B₂O₃ glass system, *J. Mol. Struct.* **1073** (2014) 164.
- [16] Sk. Mahamuda, K. Swapna, A. Srinivasa Rao, T. Sasikala, L. Rama Moorthy, Reddish-orange emission from Pr³⁺ doped zinc alumina bismuth borate glasses, *Physica B* **428** (2013) 36.
- [17] Danilo Manzani, David Pabœuf, Sidney J.L. Ribeiro, Philippe Goldner, Philippe Bretenaker, Orange emission in Pr³⁺-doped fluorindate glasses, *Opt. Mater.* **35** (2013) 383–386.
- [18] Melinda Olivier, Parastesh Pirasteh, Jean-Louis Doualan, Patrice Camy, Herve Lhermite, Jean-Luc Adam, Virginie Nazabal, Pr³⁺-doped ZBLA fluoride glasses for visible laser emission, *Opt. Mater.* **33** (2011) 980.
- [19] Joanna Pisarska, Optical properties of lead borate glasses containing Dy³⁺ ions, *J. Phys.: Condens. Matter* **21** (2009) 285101.
- [20] V. Naresh & S. Buddhudu, Analysis of energy transfer based emission spectra of (Sm³⁺, Dy³⁺): Li₂O-LiF-B₂O₃-CdO glasses, *J. Lumin.* **147** (2014) 63.
- [21] Fei Wang, Baojie Chen, Edwin Yue-Bun Pun, Hai Lin, Dy³⁺ doped sodium-magnesium-aluminum-phosphate glasses for greenish-yellow waveguide light sources, *J. Non-Cryst. Solids* **391** (2014) 17.
- [22] Kamel Damak, El Sayed Yousef, Christian Rüssel, Ramzi Maalej, White light generation from Dy³⁺ doped tellurite glass, *J. Quant. Spectrosc. Radiat. Transfer* **134** (2014) 55–63.
- [23] Raghda Saeif Eddin Said Dawaud, Suhairul Hashim, Yasser Saleh Mustafa Alajerami, M.H.A. Mhareb, N. Tamchek, Optical and structural properties of lithium sodium borate glasses doped Dy³⁺ ions, *J. Mol. Struct.* **1075** (2014) 113.
- [24] Sk. Mahamuda, K. Swapna, P. Packiyaraj, A. Srinivasa Rao, G. Vijaya Prakash, Lasing potentialities and white light generation capabilities of Dy³⁺ doped oxy-fluoroborate glasses, *J. Lumin.* **153** (2014) 382.